"It's kind of interesting to show that the strange features of quantum mechanics are actually observed. We still don't totally understand what it means."

-Leonard Mandel (1927-Feb. 8, 2001)

"Mandel seemed to be especially adept at doing experiments that were flabbergasting."

-W. Phillips (Nobel, 1997)

Run it backwards: $UV \rightarrow IR + IR$

No classical explanation. QM: Vacuum modes stimulate process

$$H = \hbar\omega_p\left(n_p + \frac{1}{2}\right) + \hbar\omega_s\left(n_s + \frac{1}{2}\right) + \hbar\omega_i\left(n_i + \frac{1}{2}\right) + H_i$$

$$H_i \sim X^{(2)}\left(a_p - a^{\dagger}{}_p\right)\left(a_s - a^{\dagger}{}_s\right)\left(a_i - a^{\dagger}{}_i\right)$$

Eight terms $\Rightarrow$ many vanish $\rightarrow$ Do not conserve energy

$$a_p a_s{}^{\dagger} a_i{}^{\dagger} \Rightarrow \omega_p \Rightarrow \omega_s + \omega_i$$

$$a_p{}^{\dagger} a_s a_i \Rightarrow \omega_s + \omega_i \Rightarrow \omega_p$$

Treat pump classically: $a_p \rightarrow \varepsilon_p e^{-i\omega_p t}$

$$H^i = \hbar G_0\left[a_s{}^{\dagger} a_1{}^{\dagger} e^{-i\omega_p t} + h.c.\right]$$

$$G_0 = \sqrt{\omega_s\omega_i}\,\frac{2\pi}{n_s n_i}\,\varepsilon_p \chi^{(2)}\left(\omega_p, \omega_s, \omega_i\right)\frac{\sin\left(\frac{\Delta kl}{2}\right)}{\frac{\Delta kl}{2}}$$

Use $\frac{dO}{dt} = \frac{-i}{\hbar}\left[O,H\right] \Rightarrow \left[a_s^{\dagger},H\right],\left[a_i^{\dagger},H\right]$

$$\Rightarrow a_s^{\dagger}(t) = \left[a_s^{\dagger}(0)\cosh G_0 t + i a_i^{\dagger}(0)\sinh G_0 t\right] e^{i\omega_s t}$$

$$\Rightarrow a_i^{\dagger}(t) = \left[a_i^{\dagger}(0)\cosh G_0 t - i a_s^{\dagger}(0)\sinh G_0 t\right] e^{-i\omega_i t}$$

$$\left\langle n_s(t)\right\rangle = \left\langle n_s(0)\right\rangle \cosh^2 G_0 t + \left[\left\langle n_i(0)\right\rangle + 1\right] sinh^2 G_0 t$$

$$\left\langle n_i(t)\right\rangle = \left\langle n_i(0)\right\rangle \cosh^2 G_0 t + \left[\left\langle n_s(0)\right\rangle + 1\right] sinh^2 G_0 t$$

Response even with no input due to vacuum fluctuations (exactly because $\left[a,a^{\dagger}\right]=1$)

For $G_0 t$ small, with no input photons, $\left|\Psi^{(t)}\right\rangle = \left|0\right\rangle + iG_0 t\left|1,1\right\rangle - \frac{(G_0 t)^2}{2}\left|2,2\right\rangle + \ldots$

$$P(1,1) = (G_0 t)^2 = \left(\frac{G_o L_n}{c}\right)^2$$

Crystal requirements:

Need non-centro-symmetric crystal (centrosymmetric crystal has $\chi_{ijk} = 0 \Rightarrow$ Need to go for $\chi^{(3)}_{ijkl}$)

All systems have $\chi^{(3)}$ but it's even smaller (well, not smaller than 0!)

Usually need birefringent crystal, in order to have phase-matching (momentum conservation) in the presence of crystal dispersion:

$K_p = K_s + K_i \rightarrow \omega_p n(\omega_p)/c = \omega_s n(\omega_s)/c + \omega_i n(\omega_i)/c$ (using $v = c/n = \omega/k$)

E.g., for degenerate SPDC, $\omega_s = \omega_i = \omega_p/2$,

$\omega_p n(\omega_p) = \omega_p n(\omega_s)/2 + \omega_p n(\omega_i)/2 \rightarrow n(\omega_p) = n(\omega_s)/2 + n(\omega_i)/2$.
This is only true if the index doesn't depend on the frequency/ wavelength.

To compensate this, we use crystals that have different index of refraction for ordinary and extraordinary polarized light:
E.g., $n_e(\omega_p) = n_o(\omega_s)/2 + n_o(\omega_i)/2$

VOLUME 25, NUMBER 2 PHYSICAL REVIEW LETTERS 13 JULY 1970

OBSERVATION OF SIMULTANEITY IN PARAMETRIC PRODUCTION OF OPTICAL PHOTON PAIRS

David C. Burnham and Donald L. Weinberg
National Aeronautics and Space Administration Electronics Research Center, Cambridge, Massachusetts 02142

(Received 12 May 1970)

The quantum mechanical description of parametric fluorescence is the splitting of a single photon into two photons. This description has been verified by observing coincidences between photons emitted by an ammonium dihydrogen phosphate crystal pumped by a 325-nm He-Cd laser. The coincidence rate R_C decreases to the calculated accidental rate [$<0.03R_C$(max)], unless the two detectors are arranged to satisfy energy and momentum conservation and have equal time delays.

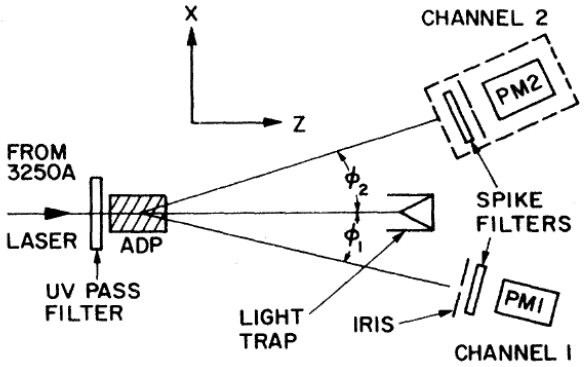

FIG. 1. Experimental arrangement. All components except the aperture in channel 1 are nominally centered on the horizontal (XZ) plane. There are sharp-cut filters in each channel to suppress scattered uv light and fluorescence. Channel 1: The aperture is located 1.00 m from the center of the crystal, and can be translated in the transverse (XY) plane. The spike filter has peak transmittance of 74% at 633 nm, and 4.0-nm pass band. The photomultiplier is an Amperex 56TUVP, with S-20 cathode apertured to 25 mm diam, and dark counting rate of 1600 sec^{-1}. Channel 2: The upper dashed-line box is symbolic. The actual arrangement is shown in the lower dashed-line box. A 95-mm focal length lens, 1.1 m from the crystal, images the pump beam position in the crystal onto the entrance slit of a $\frac{1}{4}$-m Jarrell-Ash monochromator. The beam emerging from the exit slit travels 50 mm and then strikes the photocathode of an FW-130 photomultiplier, an S-20 type, with 35-sec^{-1} dark counting rate, whose sensitive cathode area is only 1 mm in diameter. The effective aperture at the lens is therefore 2 mm in diameter. The monochrometer slits are 0.5 mm wide, giving a bandwidth of 1.5 nm.

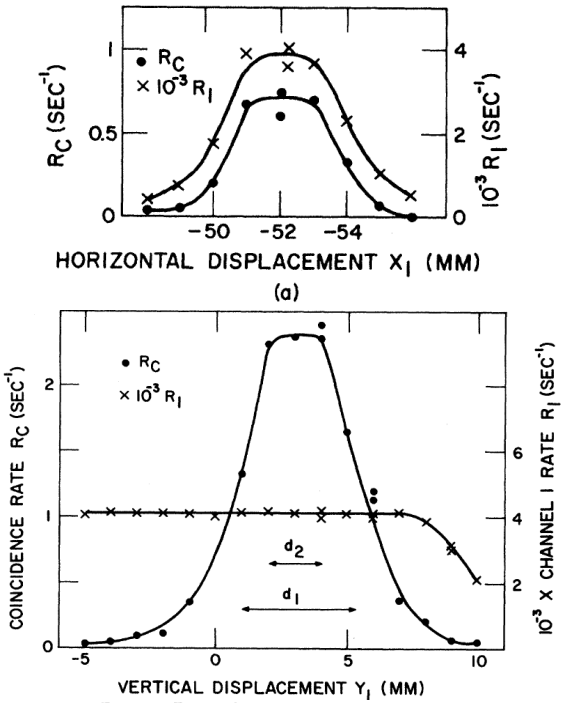

FIG. 2. R_C and R_1 as functions of position of aperture 1, for $\lambda_2 = 668.5$ nm and time delay $\tau = 0$; counting time 100 sec. (a) Horizontal (X_1) scan for $Y_1 = 0$. The pump beam position is $X_1 = 0$. (b) Vertical (Y_1) scan for $X_1 = -52$ mm. The nominal plane of the apparatus is $Y_1 = 0$. The aperture diameters, $d_1 = 4.3$ and $d_2 = 2$ mm for the two channels, are illustrated. $R_2 = 260$ sec^{-1}. Here R_1 and R_2 have been corrected for dark counts. R_C has not been corrected for the calculated accidental counting rate [0.06 sec^{-1} in (b) in the range where R_1 is constant].

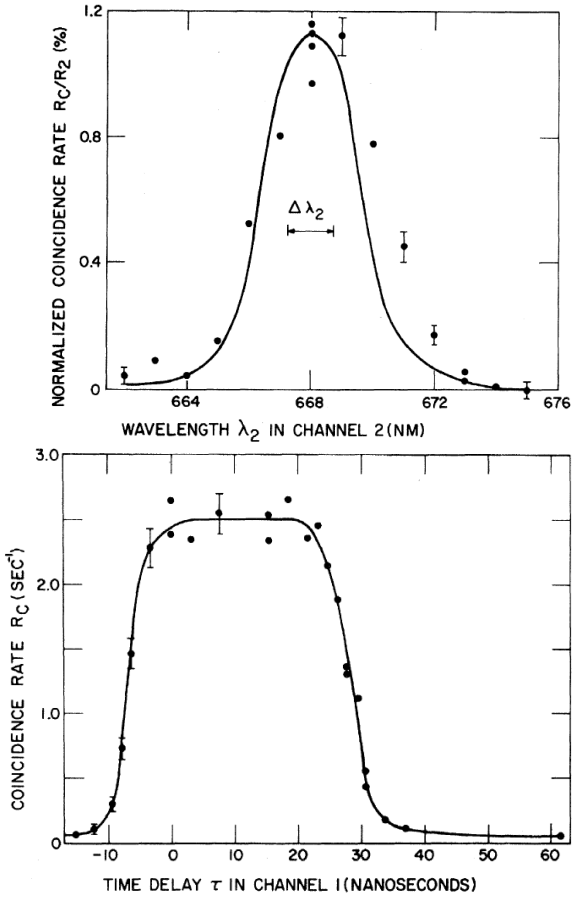

FIG. 4. R_1 vs delay τ in channel 1. The delays are introduced by adding cables between the amplifiers and discriminators. The width of the plateau is 35 ± 2 nsec full width at half-maximum. The asymmetry of the curve center about $\tau = 0$ results from different transit times in the dissimilar photomultipliers and amplifiers. No correction has been made for the calculated accidental coincidence rate, 0.05 sec^{-1}. $R_1 = 3600$ and $R_2 = 250$ sec^{-1}, with dark counts subtracted. $\lambda_2 = 668.5$, $X_1 = -52$, and $Y_1 = 3$ mm.

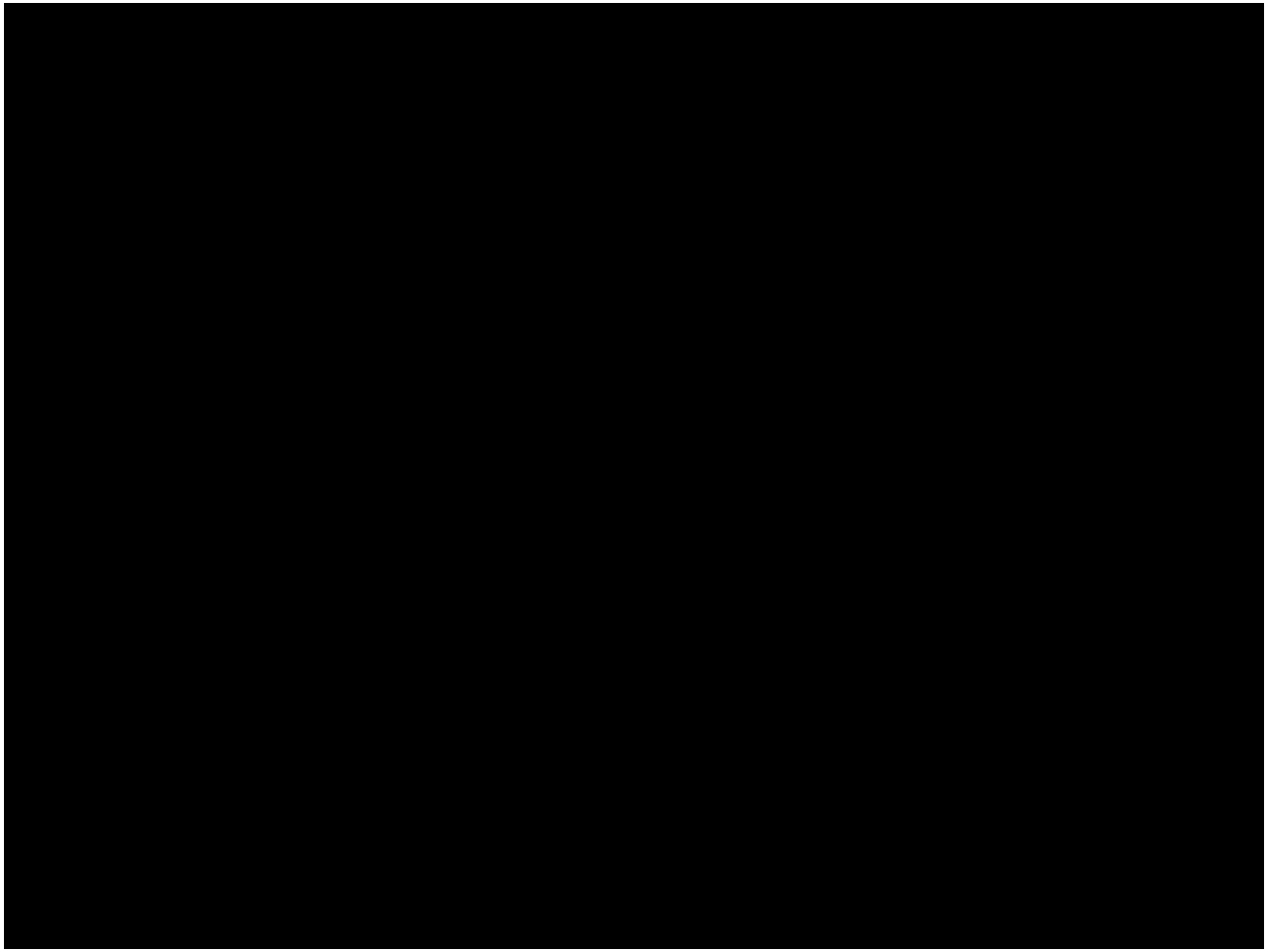

Measurement of Time Delays in the Parametric Production of Photon Pairs

S. Friberg, C. K. Hong, and L. Mandel
Department of Physics and Astronomy, University of Rochester, Rochester, New York 14627
(Received 13 December 1984)

The spread in time intervals between the two photons produced in the process of spontaneous parametric down-conversion in a potassium dihydrogen phosphate crystal has been measured with a time resolution of the order of 100 psec. The correlation time is found to be independent of the coherence time of the pump photons or of the propagation time through the crystal, consistent with recent theoretical predictions.

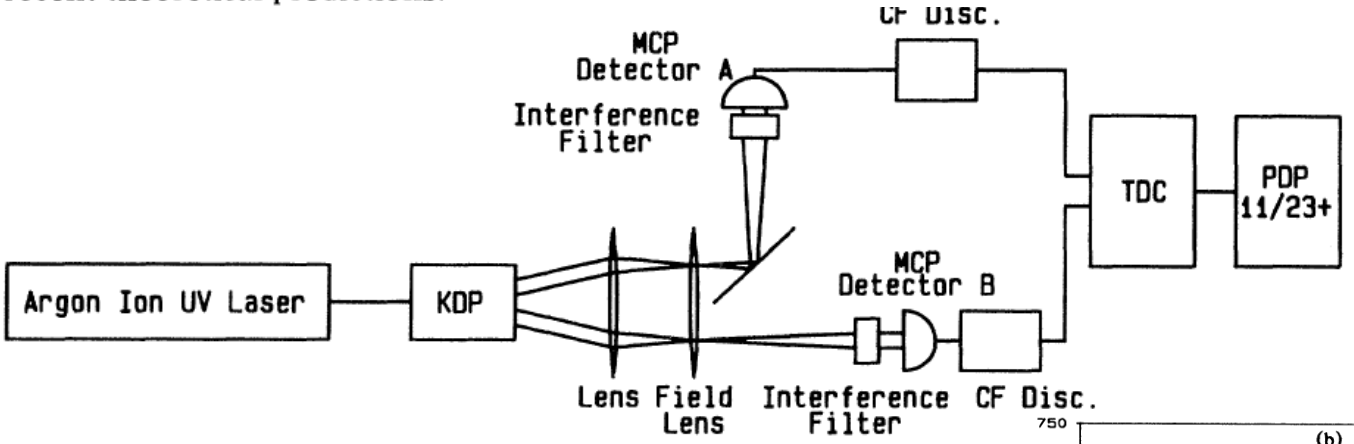

Outline of the apparatus.

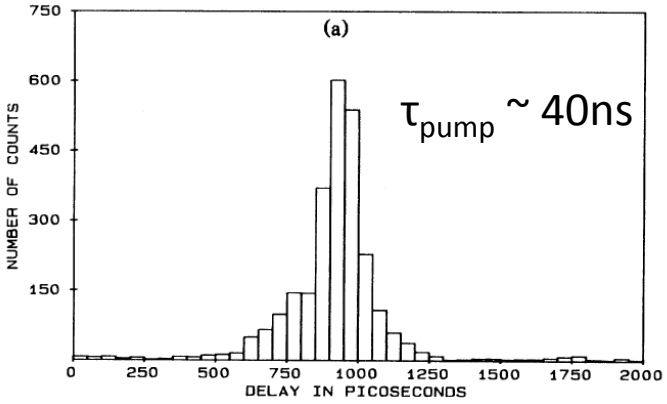

$\tau_{pump} \sim 40ns$

$\tau_{KDP} \sim 400$ ps

$\tau_{SPDC} \sim 175$ ps

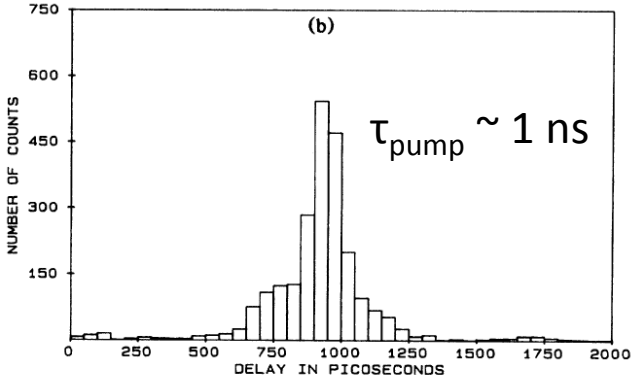

$\tau_{pump} \sim 1$ ns

FIG. 2. The measured time-delay distributions (a) for a single-mode laser (number of correlated photon pairs detected is 2542), and (b) for a multimode laser (number of correlated photon pairs detected is 2301).

Measurement of Subpicosecond Time Intervals between Two Photons by Interference

C. K. Hong, Z. Y. Ou, and L. Mandel

Department of Physics and Astronomy, University of Rochester, Rochester, New York 14627

A fourth-order interference technique has been used to measure the time intervals between two photons, and by implication the length of the photon wave packet, produced in the process of parametric down-conversion. The width of the time-interval distribution, which is largely determined by an interference filter, is found to be about 100 fs, with an accuracy that could, in principle, be less than 1 fs.

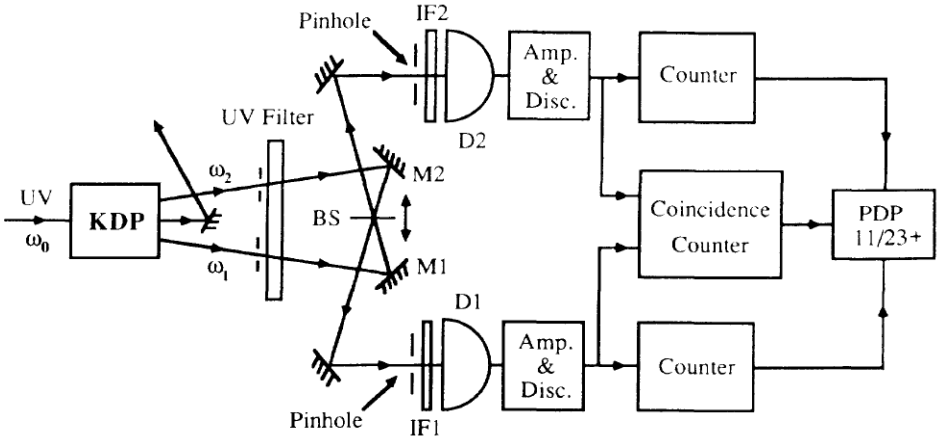

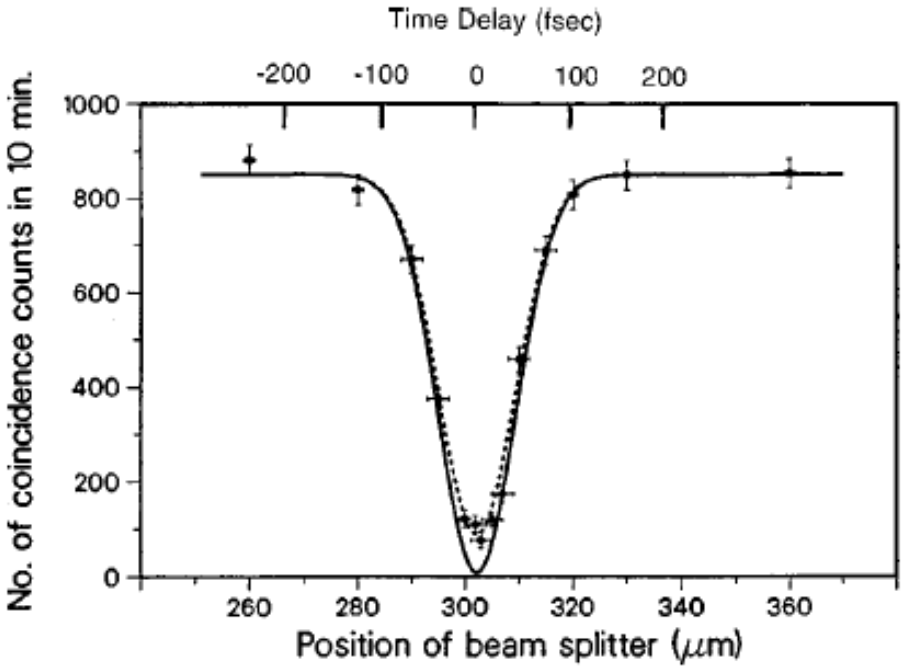

FIG. 2. The measured number of coincidences as a function of beam-splitter displacement $c\,\delta\tau$, superimposed on the solid theoretical curve derived from Eq. (11) with $R/T=0.95$, $\Delta\omega=3\times10^{13}$ rad s^{-1}. For the dashed curve the factor $2RT/(R^2+T^2)$ in Eq. (11) was multiplied by 0.9. The vertical error bars correspond to one standard deviation, whereas horizontal error bars are based on estimates of the measurement accuracy.

Measurement of the Single-Photon Tunneling Time

A. M. Steinberg, P. G. Kwiat, and R. Y. Chiao
Department of Physics, University of California, Berkeley, California 94720
(Received 5 January 1993)

Using a two-photon interferometer, we have measured the time delay for a photon to tunnel across a barrier consisting of a 1.1-μm-thick 1D photonic band-gap material. The peak of the photon wave packet appears on the far side of the barrier 1.47 ± 0.21 fs *earlier* than it would if it were to travel at the vacuum speed of light c. Although the apparent tunneling velocity $(1.7 \pm 0.2)c$ is superluminal, this is not a genuine signal velocity, and Einstein causality is not violated. The measured tunneling time is consistent with the group delay ("phase time"), but not with the semiclassical time.

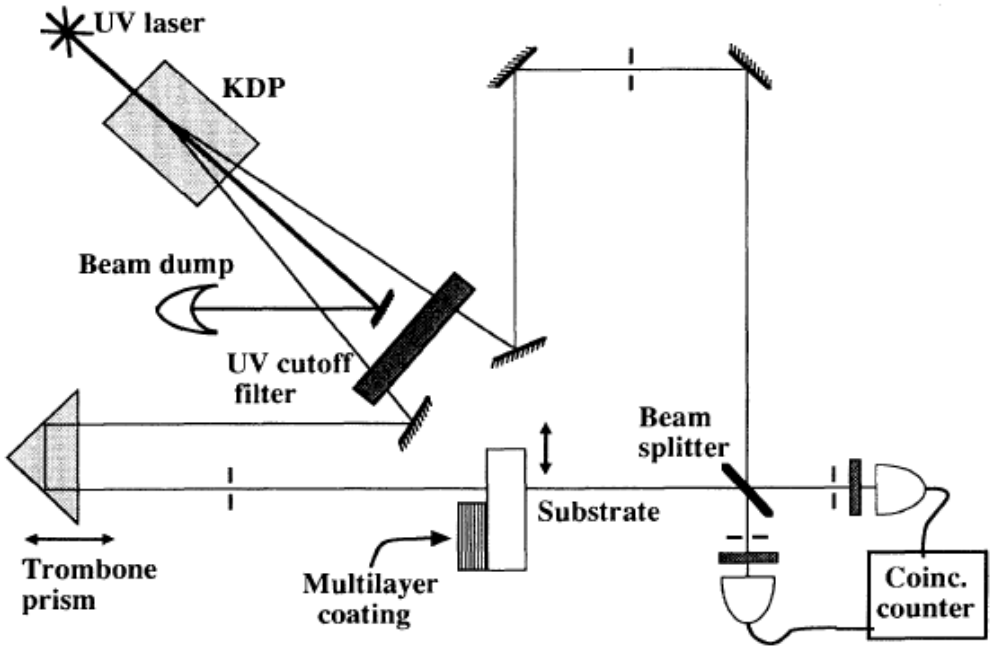

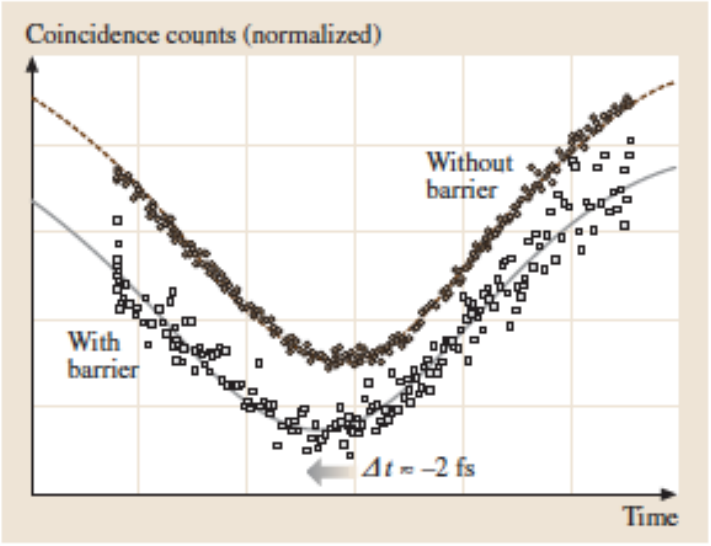

Fig. 80.12 Coincidence profiles with and without the tunnel barrier map out the single-photon wave packets. The *lower profile* shows the coincidences with the barrier; this profile is shifted by ≈ 2 fs to negative times relative to the one with no barrier (*upper curve*): the average particle which tunnels arrives earlier than the one which travels the same distance in air

Ultrabroadband Biphotons Generated via Chirped Quasi-Phase-Matched Optical Parametric Down-Conversion

Magued B. Nasr,[1] Silvia Carrasco,[1] Bahaa E. A. Saleh,[1] Alexander V. Sergienko,[1] Malvin C. Teich,[1] Juan P. Torres,[2] Lluis Torner,[2] David S. Hum,[3] and Martin M. Fejer[3]

[1]*Quantum Imaging Laboratory**, *Departments of Electrical & Computer Engineering and Physics, Boston University, Boston, Massachusetts 02215, USA*

[2]*ICFO-Institut de Ciencies Fotoniques, and Department of Signal Theory and Communications, Universitat Politecnica de Catalunya, Mediterranean Technology Park, 08860 Castelldefels (Barcelona), Spain*

[3]*E. L. Ginzton Laboratory, Stanford University, Stanford, California 94305, USA*

(Received 12 December 2007; published 5 May 2008; publisher error corrected 6 May 2008)

We generate ultrabroadband biphotons via the process of spontaneous parametric down-conversion (SPDC) in quasi-phase-matched nonlinear gratings that have a linearly chirped wave vector. By using these ultrabroadband biphotons (300-nm bandwidth), we measure the narrowest Hong-Ou-Mandel dip to date, having a full width at half maximum of 7.1 fs. This enables the generation of a high flux of nonoverlapping biphotons with ultrabroad bandwidth, thereby promoting the use of SPDC light in many nonclassical applications.

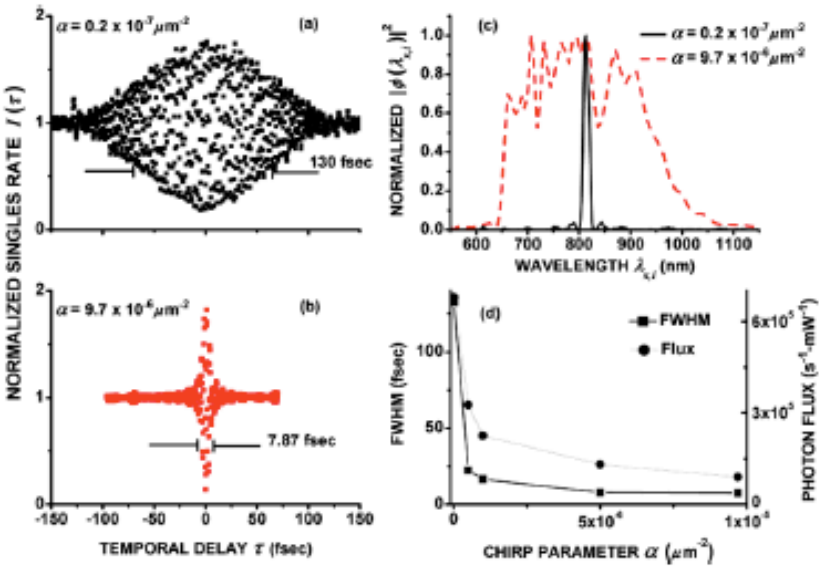

FIG. 2 (color online). Normalized interferogram $I(\tau)$ for collinear SPDC. Emission from a C-PPSLT grating with (a) $\alpha = 0.2 \times 10^{-7}\ \mu\text{m}^{-2}$ exhibits a FWHM of 130 fs and (b) $\alpha = 9.7 \times 10^{-6}\ \mu\text{m}^{-2}$ exhibits a FWHM of 7.87 fs. (c) The power spectral densities $|\phi(\Omega)|^2$, plotted vs wavelength $\lambda_{s,i}$, for the data shown in (a) and (b). (d) The FWHM (squares) of the measured interferograms for gratings of different degrees of chirp are plotted on the left ordinate. The biphoton fluxes per milliwatt of pump power (circles) are plotted on the right ordinate. The lines connecting the experimental points are for guiding the eye.

Integrated quantum photonics

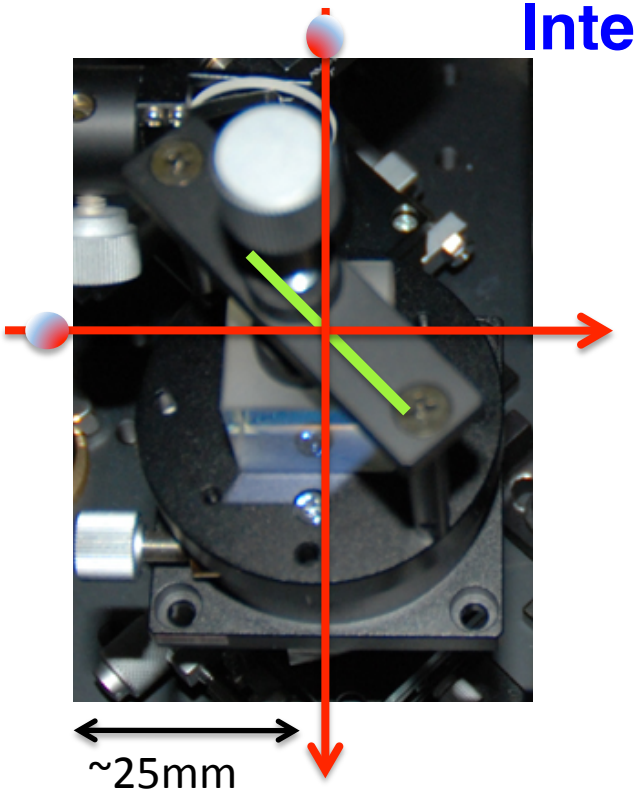

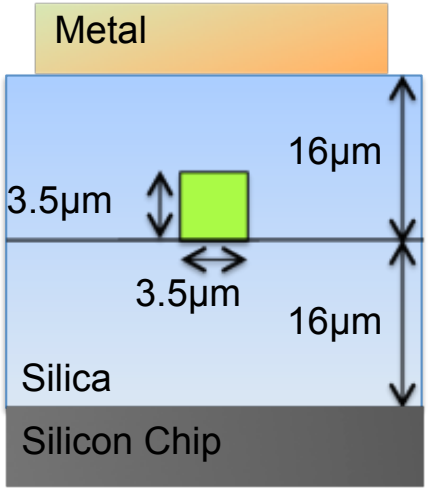

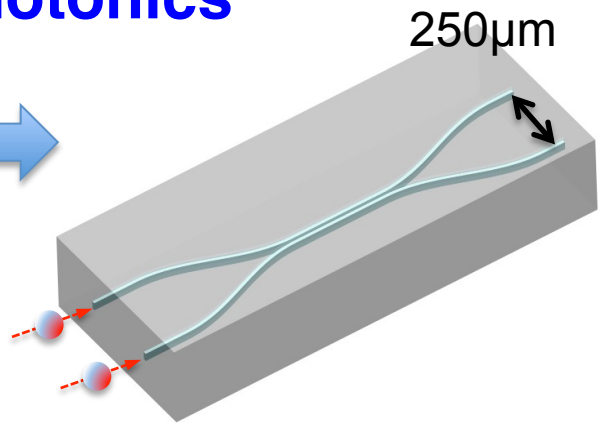

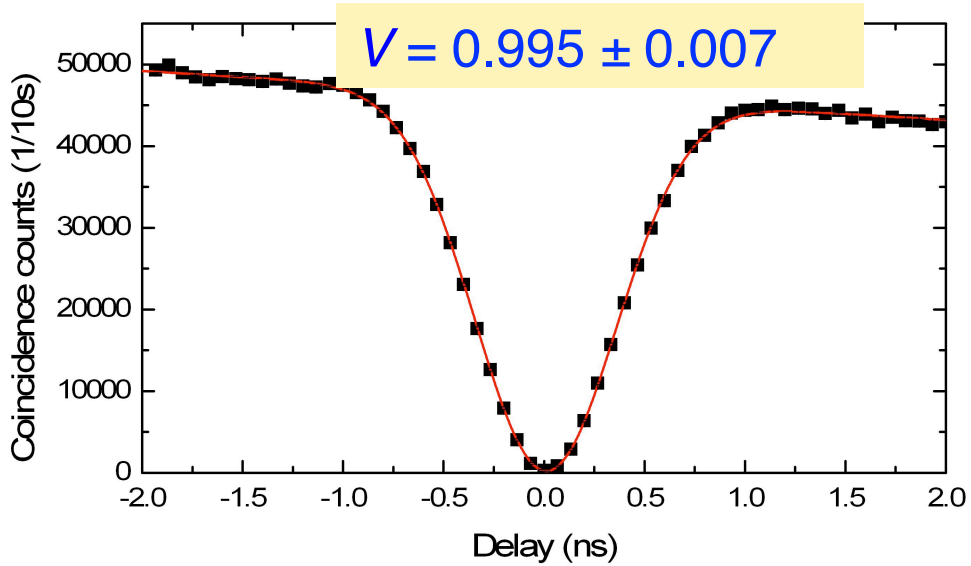

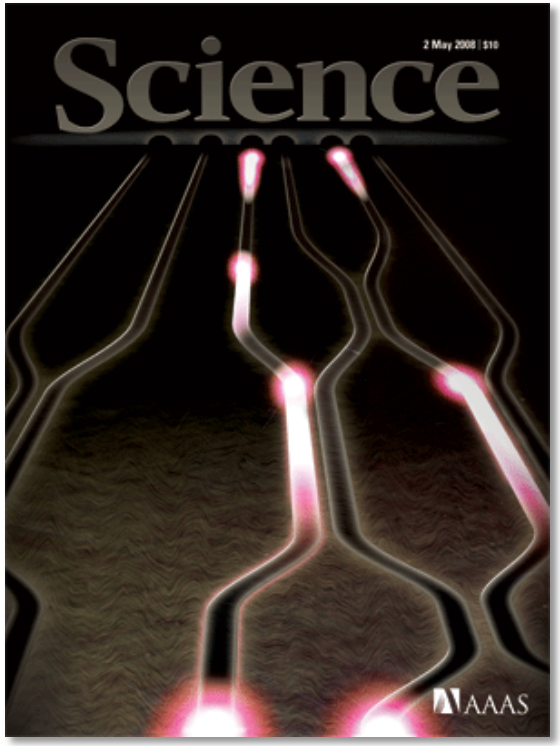

Politi, Cryan, Yu, Rarity and O'Brien
***Science* 320,** 646 (2008)

Experimental Interference of Independent Photons

Rainer Kaltenbaek and Bibiane Blauensteiner
Institute for Experimental Physics, University of Vienna, Boltzmanngasse 5, A-1090 Vienna, Austria

Marek Żukowski
Institute for Experimental Physics, University of Vienna, Boltzmanngasse 5, A-1090 Vienna, Austria and Institute of Theoretical Physics and Astrophysics, University of Gdansk, Wita Stwosza 57, PL-08-952 Gdansk, Poland

Markus Aspelmeyer and Anton Zeilinger
Institute for Experimental Physics, University of Vienna, Boltzmanngasse 5, A-1090 Vienna, Austria and Institute for Quantum Optics and Quantum Information (IQOQI), Austrian Academy of Sciences, Boltzmanngasse 3, A-1090 Vienna, Austria

(Received 7 March 2006; published 21 June 2006)

Interference of photons emerging from independent sources is essential for modern quantum-information processing schemes, above all quantum repeaters and linear-optics quantum computers. We report an observation of nonclassical interference of two single photons originating from two independent, separated sources, which were actively synchronized with a rms timing jitter of 260 fs. The resulting (two-photon) interference visibility was $(83 \pm 4)\%$.

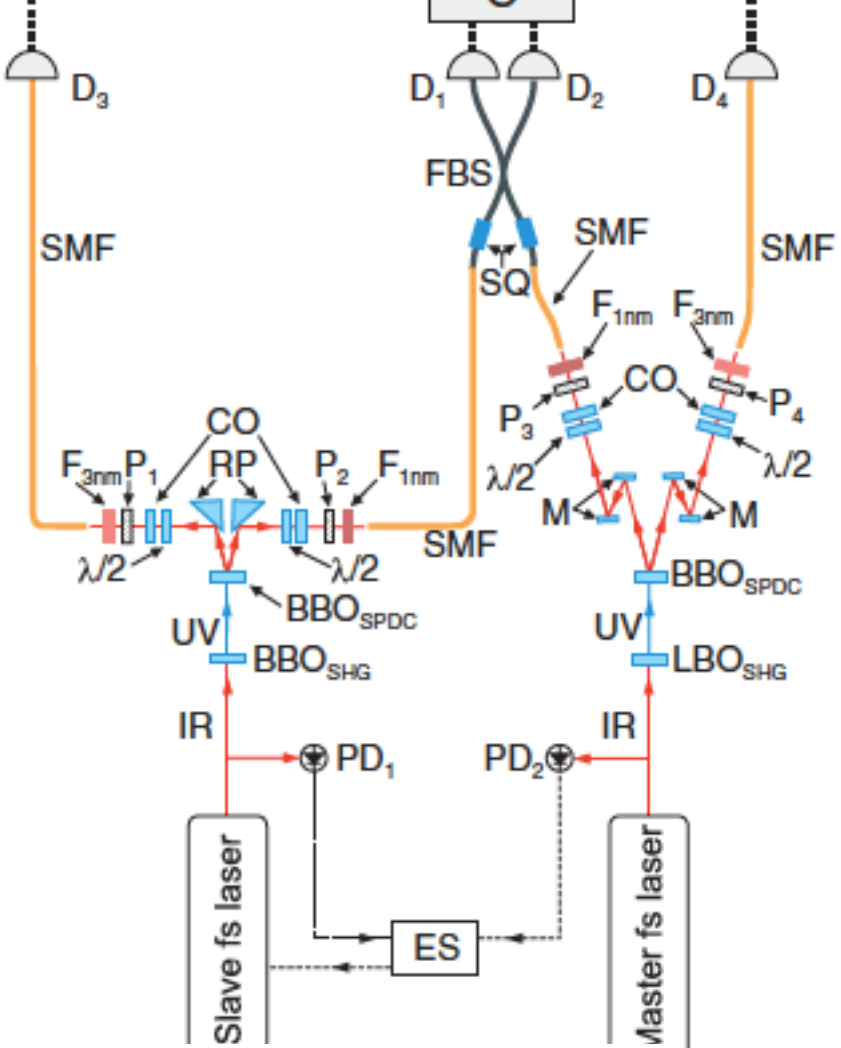

FIG. 2 (color online). Pulsed IR laser beams, which were electronically synchronized (ES, see Fig. 1), were frequency doubled [one in a lithium triborate (LBO), the other in a β-barium borate (BBO) crystal]. The resulting UV beams pumped type-II BBO crystals for SPDC. Reflecting prisms (RP) and mirrors (M) guided the SPDC photons through half-wave plates and BBO crystals (CO) to compensate various walk-off effects. All photons were coupled into single-mode fibers (SMF) to guarantee optimal spatial mode overlap. Polarizers P_1-P_4, narrow bandwidth filters F_{1nm} or F_{3nm}, and fiber squeezers (SQ) ensured the indistinguishability of the photons at the single-mode fiber beam splitter (FBS). Coincidences C between the detectors D_1 and D_2 could be triggered on detection events in both D_3 and D_4.

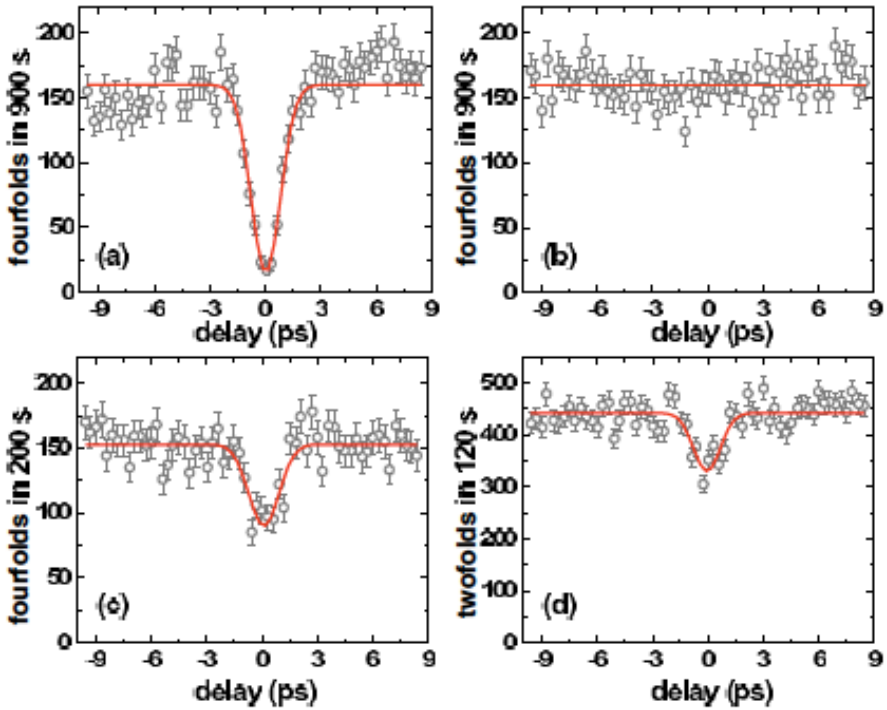

FIG. 3 (color online). Experimental two-photon interference from independent sources. The solid lines represent Gaussian fits to the data points. (a) HOM-type interference of indistinguishable photons from actively synchronized independent sources. The observed visibility was $83 \pm 4\%$ and the dip width was 0.79 ± 0.04 ps. (b) Input photons distinguishable by their polarization. No interference occurs. (c) Unpolarized input photons show limited interference due to partial distinguishability. The observed visibility was $(26 \pm 3\%)$. (d) Classical interference from a thermal source, showing a dip visibility of $15 \pm 2\%$.

Indistinguishable photons from a single-photon device

Charles Santori*, David Fattal*, Jelena Vučković*, Glenn S. Solomon & Yoshihisa Yamamoto*‡

** Quantum Entanglement Project, ICORP, JST, E. L. Ginzton Laboratory, Stanford University, Stanford, California 94305-4088, USA*

NATURE | VOL 419 | 10 OCTOBER 2002

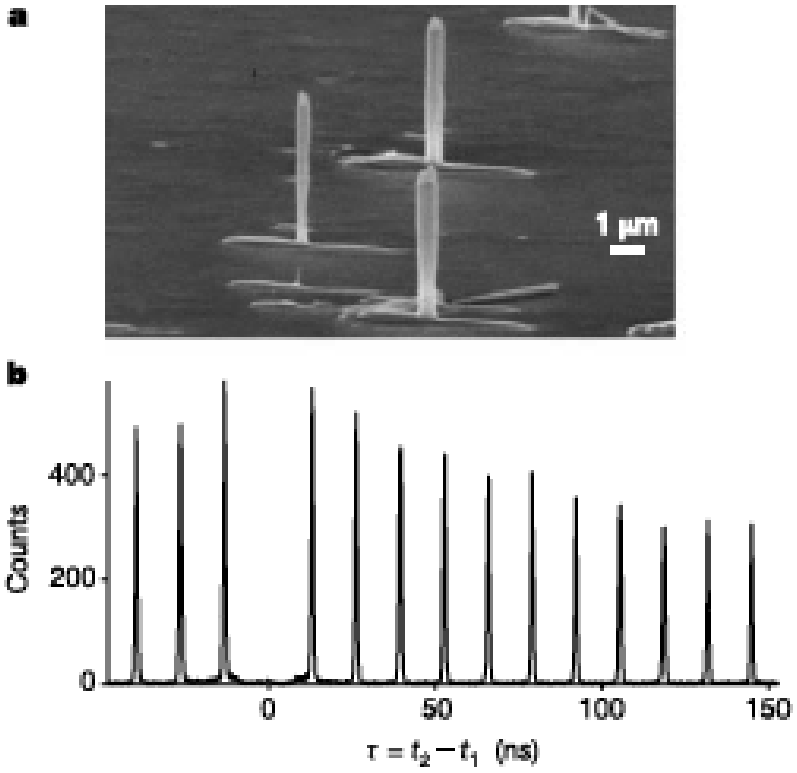

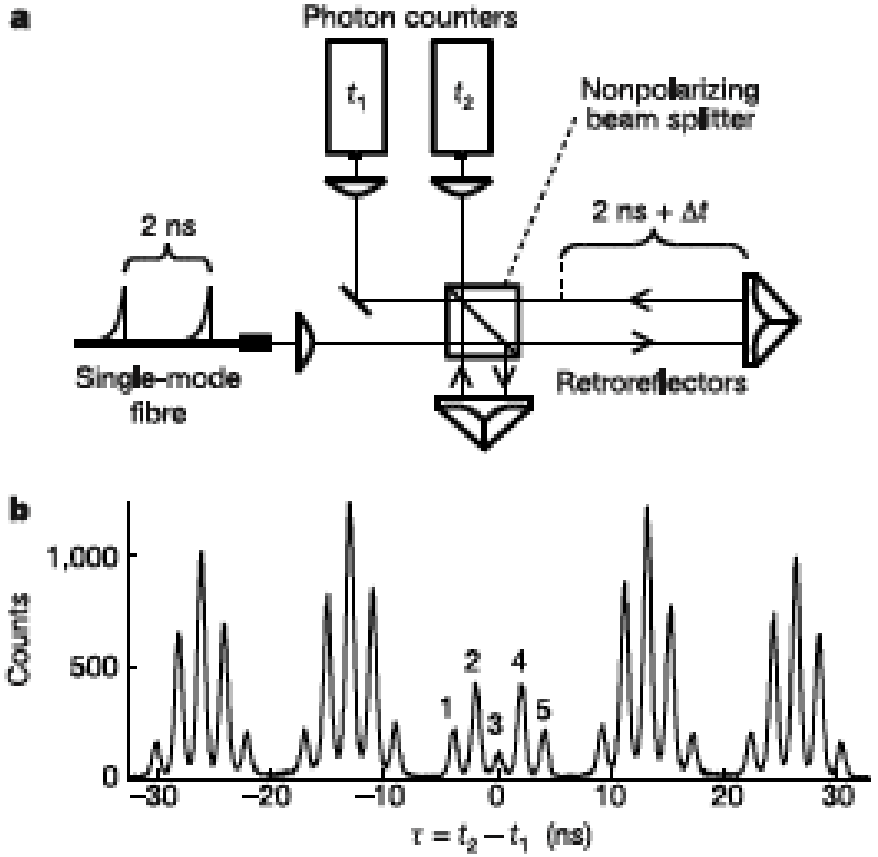

Figure 3 Two-photon interference experiment. **a**, Every 13 ns, two pulses, separated by 2 ns and containing 0 or 1 photons, arrive through a single-mode fibre. The pulses are interfered with each other using a Michelson-type interferometer with a $(2\,\text{ns} + \Delta t)$ path-length difference. Corner-cube retroreflectors are used at the ends of the arms, so that the mode overlap is insensitive to slight angular misalignment of the optical elements. The length of the short arm can be adjusted over long distances by a 15-cm motor stage. The fringe contrast measured using a laser with a long coherence length was 0.92, limited by optical surface imperfections. The interferometer outputs are collected by photon counters, and the resulting electronic signals are correlated using a time-to-amplitude converter followed by a multi-channel analyser card, which generates a histogram of the relative delay time $\tau = t_2 - t_1$ between a photon detection at one counter (t_1) and the other (t_2). **b**, Such a histogram (53-ps bin size) obtained for quantum dot 2, with $\Delta t = 0$. The number of repetitions was $N = 2.3 \times 10^{10}$ (5 min), and the combined two-photon generation and detection efficiency was $\eta^{(2)} = 2.5 \times 10^{-6}$, which includes all losses in the experimental set-up. The small area of peak 3 demonstrates two-photon interference.

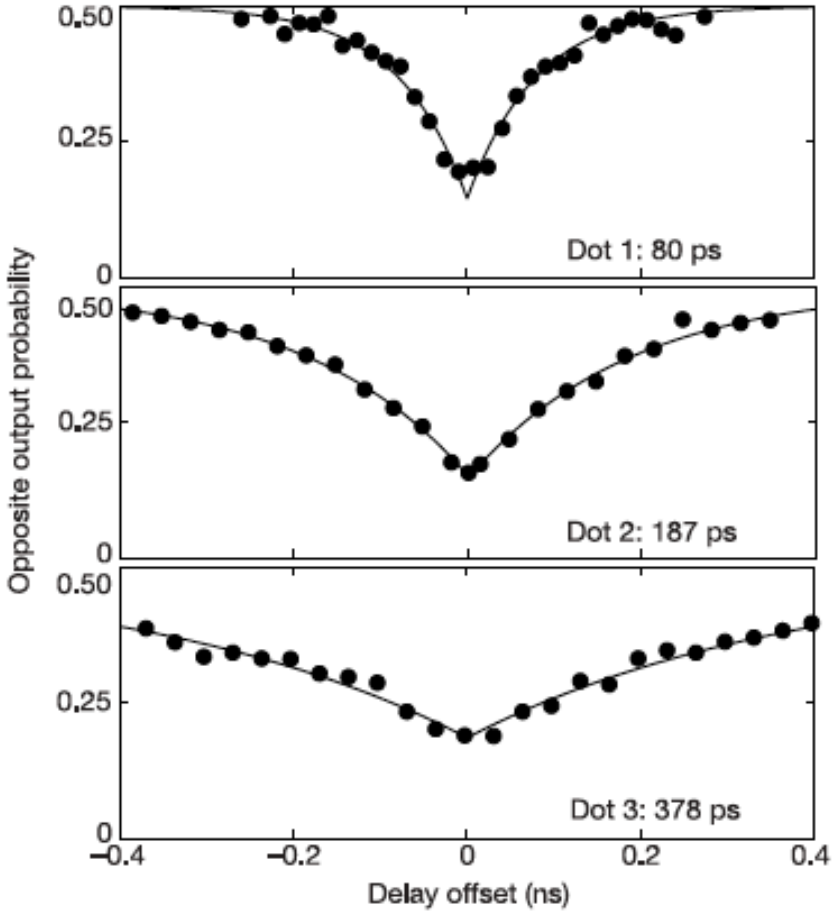

Figure 4 The probability that two photons that collide at the beam splitter leave in opposite directions, plotted as a function of interferometer delay offset, Δt. Data are shown for quantum dots 1, 2 and 3. The drops in the coincidence rate near zero offset demonstrate two-photon interference. From model fits (solid lines), the 1/e widths of the dips are estimated as 80, 187 and 378 ps for dots 1, 2 and 3, respectively, in close agreement with the measured spontaneous emission lifetimes.

Table 1 **Summary of quantum-dot parameters**

	$g^{(2)}$	g	τ_s (ps)	τ_c (ps)	τ_m (ps)	$V(0)$
Dot 1	0.053	0.039	89	48	80	0.72
Dot 2	0.067	0.027	166	223	187	0.81
Dot 3	0.071	0.025	351	105	378	0.74

For the three quantum dots chosen for this study, we show the conventional two-photon suppression parameter $g^{(2)}$, the ratio g of the probability of emitting two photons in either of two consecutive pulses to the probability of emitting one photon in each pulse, the spontaneous emission lifetime τ_s, the coherence length τ_c, the 1/e width of the Mandel dip τ_m, and the two-photon overlap at zero path-length difference $V(0)$.

On-Demand Single Photons with High Extraction Efficiency and Near-Unity Indistinguishability from a Resonantly Driven Quantum Dot in a Micropillar

Scalable photonic quantum technologies require on-demand single-photon sources with *simultaneously* high levels of purity, indistinguishability, and efficiency. These key features, however, have only been demonstrated separately in previous experiments. Here, by *s*-shell pulsed resonant excitation of a Purcell-enhanced quantum dot-micropillar system, we deterministically generate resonance fluorescence single photons which, at π pulse excitation, have an extraction efficiency of 66%, single-photon purity of 99.1%, and photon indistinguishability of 98.5%. Such a single-photon source for the first time combines the features of high efficiency and near-perfect levels of purity and indistinguishabilty, and thus opens the way to multiphoton experiments with semiconductor quantum dots.

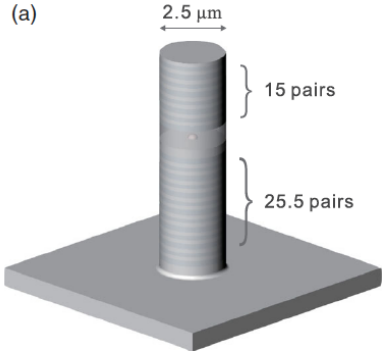

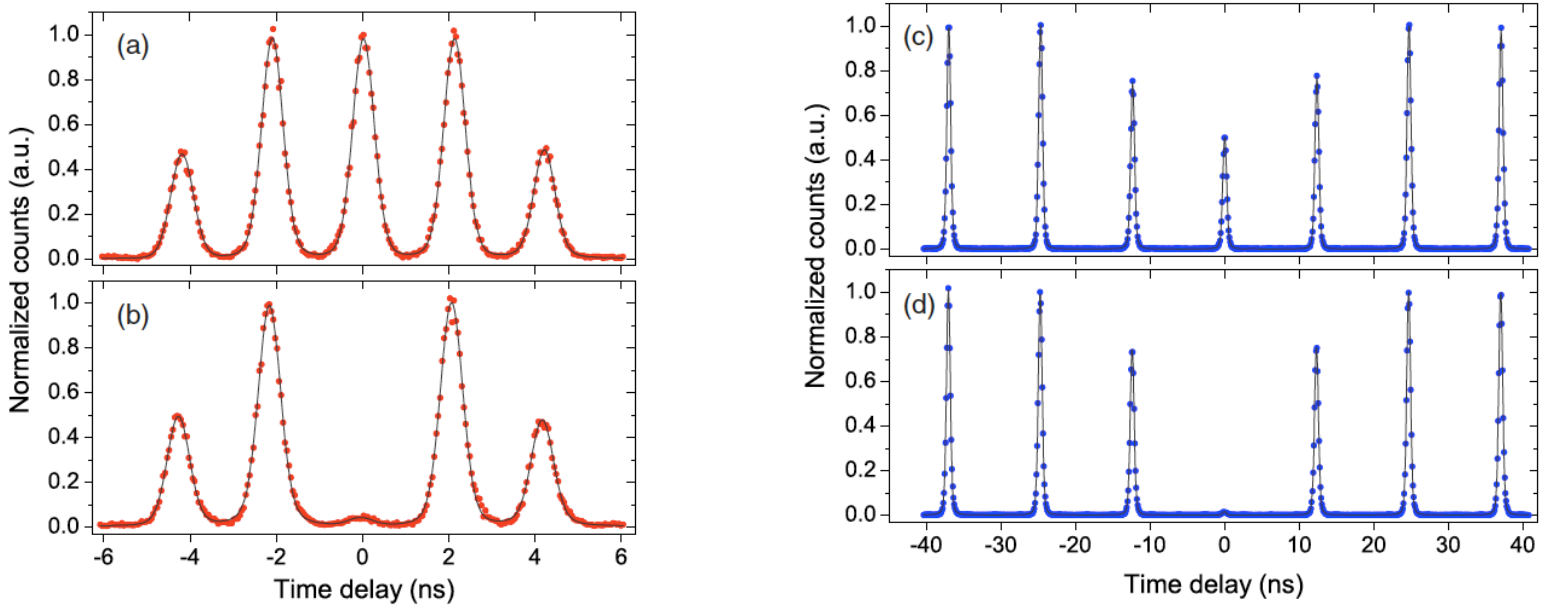

FIG. 3. Quantum interference between two pulsed RF single photons from a Purcell-enhanced QD-micropillar system. The time separation between the two single photons emitted from the single QD are set at 2.1 ns in (a)–(b) and 12.4 ns in (c)–(d), respectively. The input two photons are π-pulse excited and prepared in cross (a), (c) and parallel (b), (d) polarizations, respectively. The fitting function is the convolution of exponential decay (emitter decay response) with Gaussian (photon detection time response). The area of the fitted central peaks are extracted and used to calculate the raw visibility, which is 0.964(3) and 0.959(3) for the time delay of 2.1 and 12.4 ns, respectively. All the data points presented are raw data without background subtraction.

Interference of Single Photons from Two Separate Semiconductor Quantum Dots

Edward B. Flagg,* Andreas Muller, Sergey V. Polyakov, Alex Ling, Alan Migdall, and Glenn S. Solomon†

Joint Quantum Institute, National Institute of Standards and Technology & University of Maryland, Gaithersburg, Maryland, USA

(Received 19 January 2010; published 1 April 2010)

We demonstrate and characterize interference between discrete photons emitted by two separate semiconductor quantum dot states in different samples excited by a pulsed laser. Their energies are tuned into resonance using strain. The photons have a total coalescence probability of 18.1% and the coincidence rate is below the classical limit. Postselection of coincidences within a narrow time window increases the coalescence probability to 47%. The probabilities are reduced from unity because of dephasing and the postselection value is also reduced by the detector time response

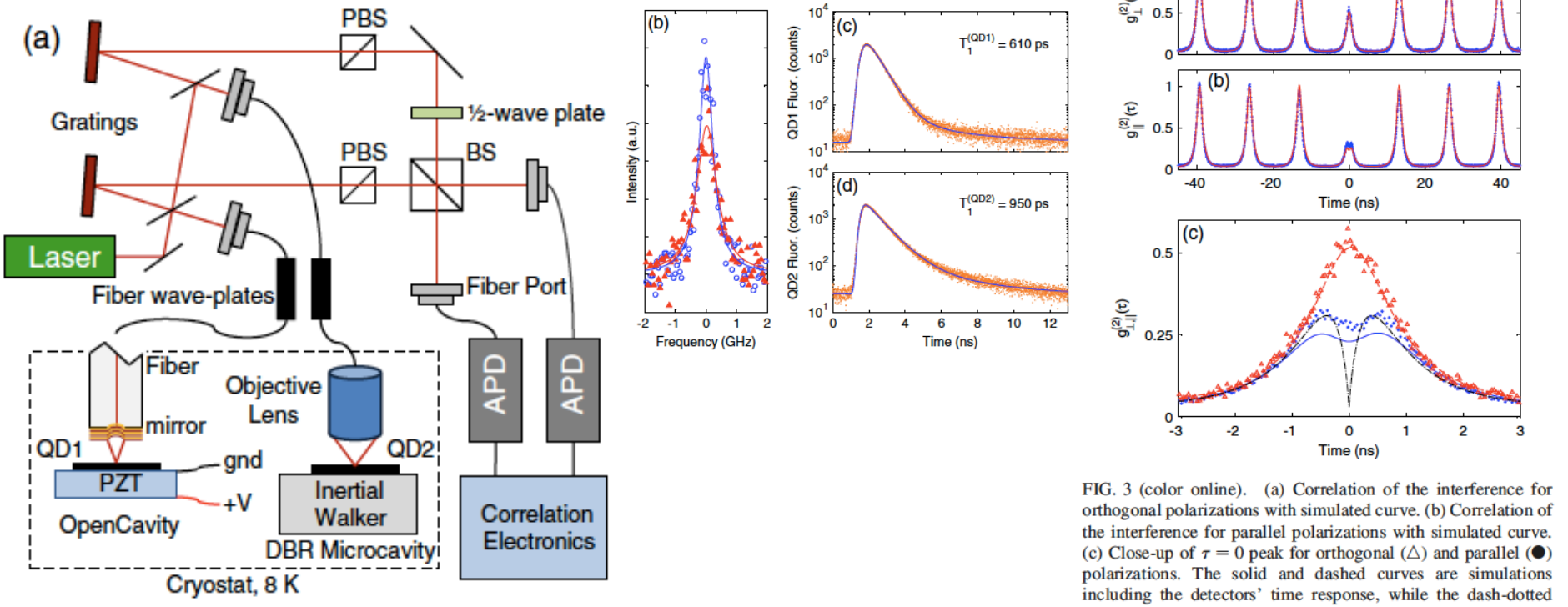

FIG. 3 (color online). (a) Correlation of the interference for orthogonal polarizations with simulated curve. (b) Correlation of the interference for parallel polarizations with simulated curve. (c) Close-up of $\tau = 0$ peak for orthogonal (△) and parallel (●) polarizations. The solid and dashed curves are simulations including the detectors' time response, while the dash-dotted curve is the expected curve for infinitely fast detectors.

Vol 440|6 April 2006|doi:10.1038/nature04628

Quantum interference between two single photons emitted by independently trapped atoms

J. Beugnon[1], M. P. A. Jones[1], J. Dingjan[1], B. Darquié[1], G. Messin[1], A. Browaeys[1] & P. Grangier[1]

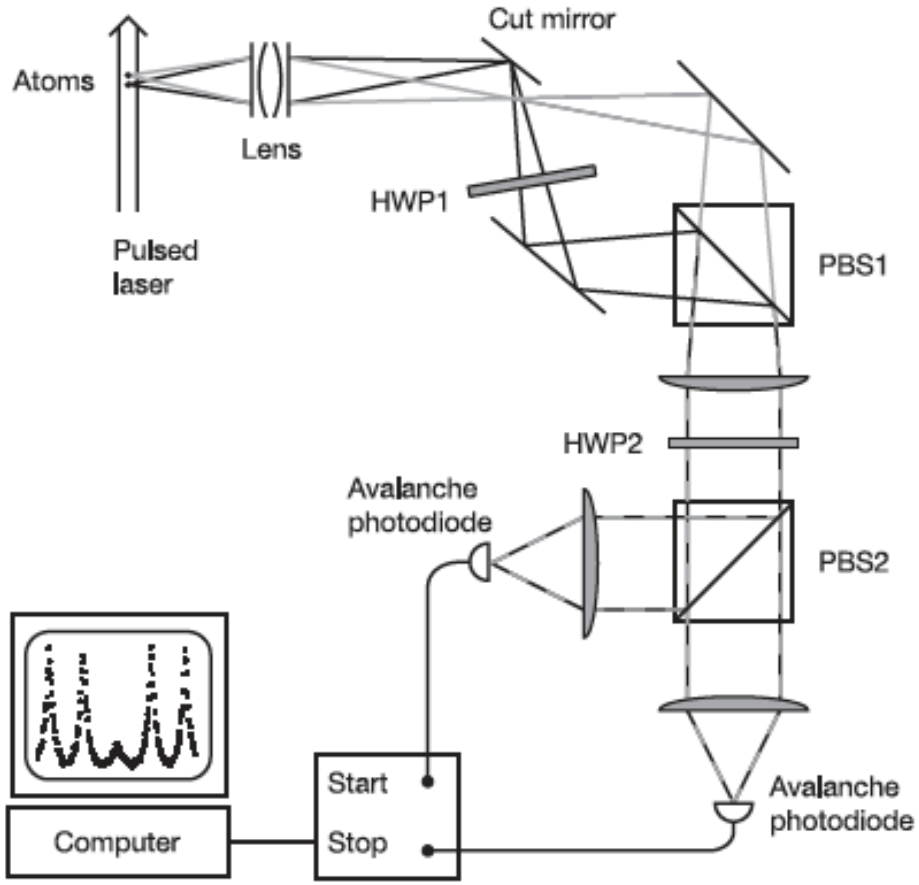

Figure 1 | Experimental set-up. The two atoms are trapped in two dipole traps separated by 6 μm, and they are excited by the same pulsed laser beam. The trap depth is 1.5 mK, and the trap frequency along the axis of the pulsed laser beam is 120 kHz. The emitted photons are collected by the same lens that is used to create the dipole traps. The light from one of the traps is separated off using a cut mirror placed close to the image plane of the objective. In the plane of the cut mirror, the spot corresponding to each trap has a waist of ~90 μm, and the two images are separated by 500 μm. The half-wave plate HWP1 is oriented such that, at polarizing beam splitter PBS1, the light beams from the two atoms are recombined into the same spatial mode, but with orthogonal polarizations. There are then two configurations to detect the photons: either the axis of HWP2 is set so that the two orthogonal incident polarizations are equally mixed in each output of PBS2, as in a 50/50 beam splitter, or the axis is set so that the polarizations are unchanged, and then PBS2 simply separates the two beams coming from the two atoms without mixing them. Two avalanche photodiodes are placed in the two output ports of PBS2. The measured overall collection and detection efficiency is 0.6% for each photodiode[21].

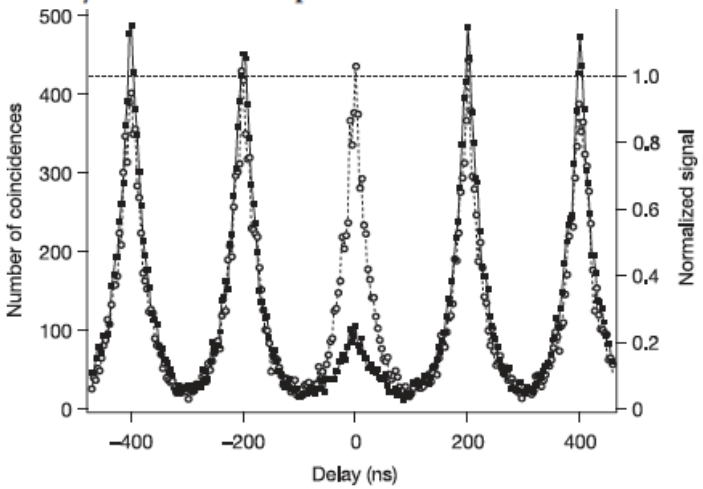

HOM interference is the 'gold-standard' to determine if two photons are indistinguishable from each other. But it's harder to set up than some other measurements….

As of a few years ago, measuring $g^{(2)}(0)$ became a very good way to characterize the purity of photons:

If a photon is entangled to some other system, than the photon won't be in a pure state. But that entanglement is enough to make the photon distinguishable from some other photon. This will reduce the HOM visibility. What does it do to $g^{(2)}$?

It reduces it from $g^{(2)} = 2$ (for a thermal state) to $g^{(2)} = 1 + 1/n$,
where n is the number of modes the photon is occupying.

You saw a special case of this in the HW: $g^{(2)}$ for a mixture of H and V polarizations was only 3/2.

Observation of a Nonclassical Berry's Phase for the Photon

Paul G. Kwiat and Raymond Y. Chiao

Coincidence detection of photon pairs produced in parametric fluorescence, in conjunction with a Michelson interferometer in which one member of each pair acquired a geometrical phase due to a cycle in polarization states, has allowed the first observation of Berry's phase at the single-photon level. We have verified that each interfering photon was essentially in an $n=1$ Fock state, by means of a beam splitter following the interferometer combined with a triple-coincidence technique. The results can be interpreted in terms of a nonlocal collapse of the wave function.

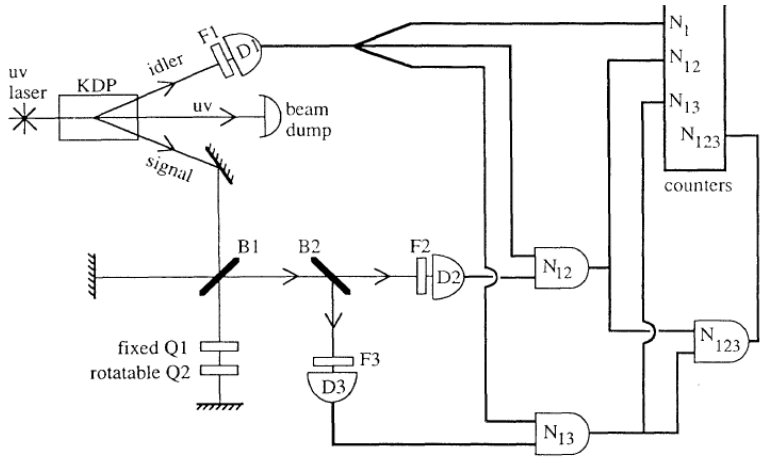

FIG. 1. Schematic of experiment to observe an optical Berry's phase on the quantum level. $D1$, $D2$, and $D3$ are photomultipliers, $Q1$ and $Q2$ quarter-wave plates, and $B1$ and $B2$ beam splitters. Logical AND symbols denote coincidence detectors.

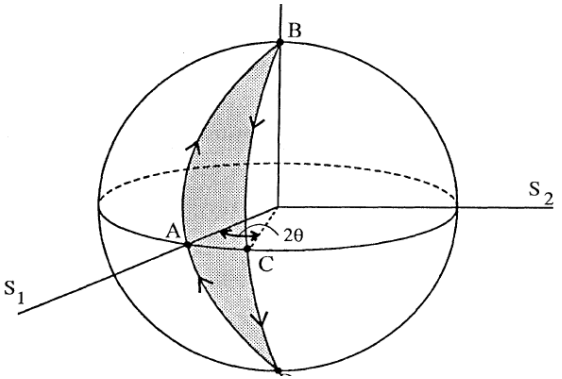

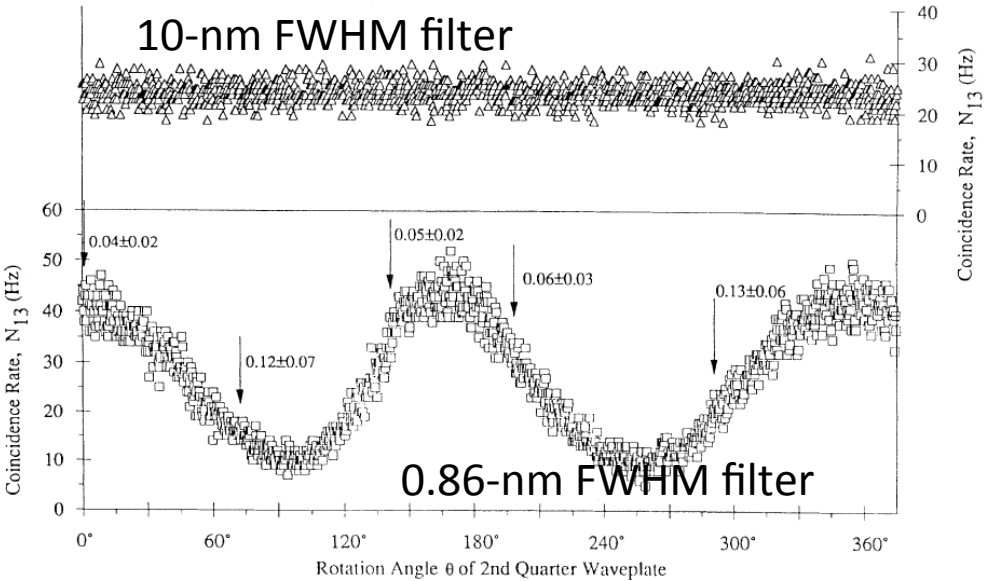

Fig. 3. Interference fringes (lower trace, squares) for an unbalanced Michelson interferometer with a slowly varying Berry's phase, observed in coincidences between *D3* and *D1* with a narrow remote filter *F1*. With a broad *F1*, these fringes disappear (upper trace, triangles). They also disappear when detected by *D3* alone. Vertical arrows indicate where the anticorrelation parameter α was measured.

Observation of Nonclassical Effects in the Interference of Two Photons

R. Ghosh and L. Mandel

Department of Physics and Astronomy, University of Rochester, Rochester, New York 14627

(Received 21 May 1987)

By measuring the joint probability for the detection of two photons at two points as a function of the separation between the points, we have demonstrated the existence of nonclassical effects in the interference of signal and idler photons in parametric down-conversion. In principle, the detection of one photon at one point rules out certain positions where the other photon can appear.

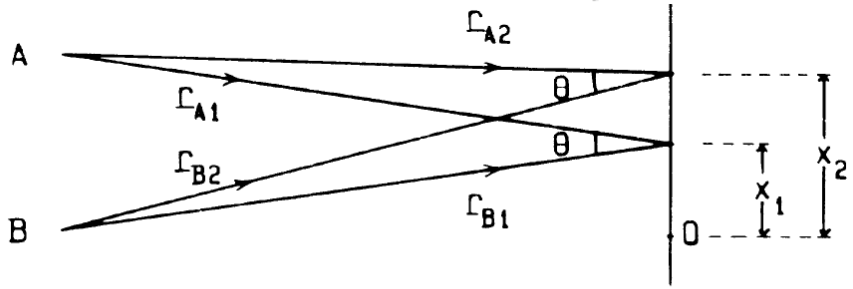

FIG. 1. The geometry of the interference experiment.

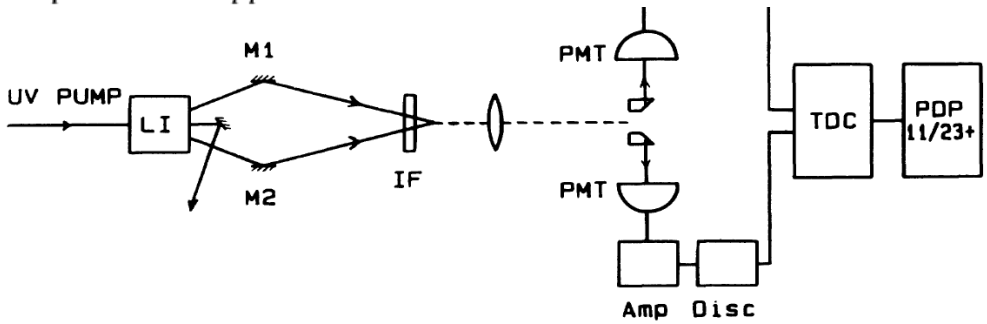

FIG. 2. Outline of the apparatus.

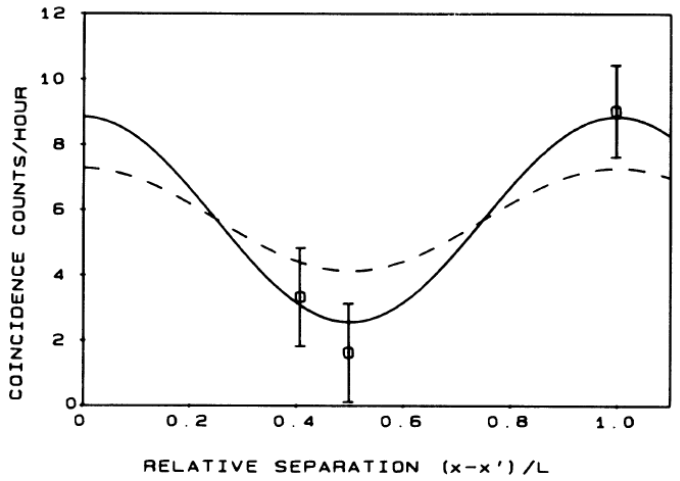

FIG. 3. Experimental results superimposed on the predictions of quantum theory given by Eq. (9) (full curve), and of the classical theory with maximum modulation (dashed curve).

Evidence for phase memory in two-photon down conversion through entanglement with the vacuum

Z. Y. Ou, L. J. Wang, X. Y. Zou, and L. Mandel
Department of Physics and Astronomy, University of Rochester, Rochester, New York 14627
(Received 14 August 1989)

An experiment has been carried out in which two pairs of light beams produced by down conversion in two nonlinear crystals driven by a common pump were mixed by two beam splitters, and the coincidence rate for simultaneous detections of mixed signal and idler photons was measured. It is found that the down-converted light carries information about the phase of the pump field through the entanglement of the down-converted photons with the vacuum.

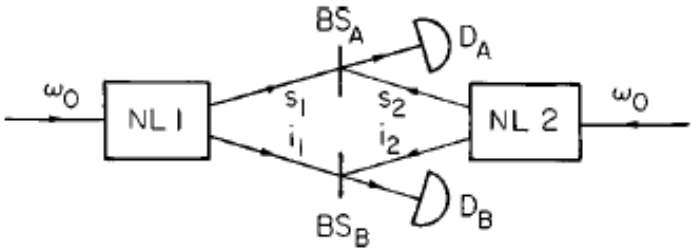

FIG. 3. Principle of the interference experiment with two downconverters in which both one-photon and two-photon interference can be investigated (after Ou *et al.*, 1990).

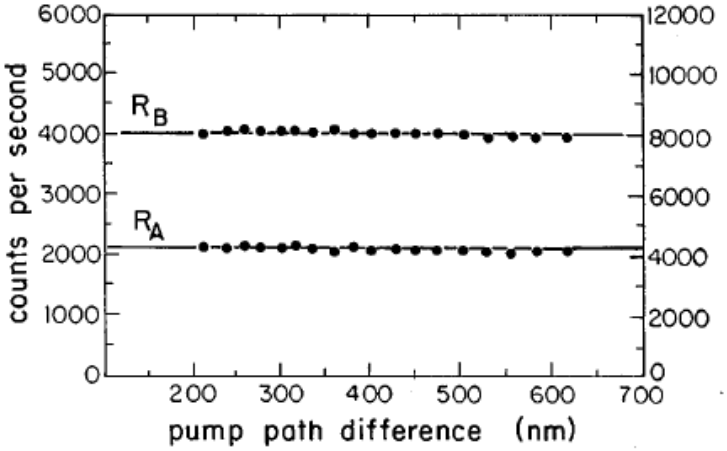

FIG. 4. Results of measurements of the photon counting rate by D_A and D_B in Fig. 3 as a function of path difference, showing the absence of one-photon interference.

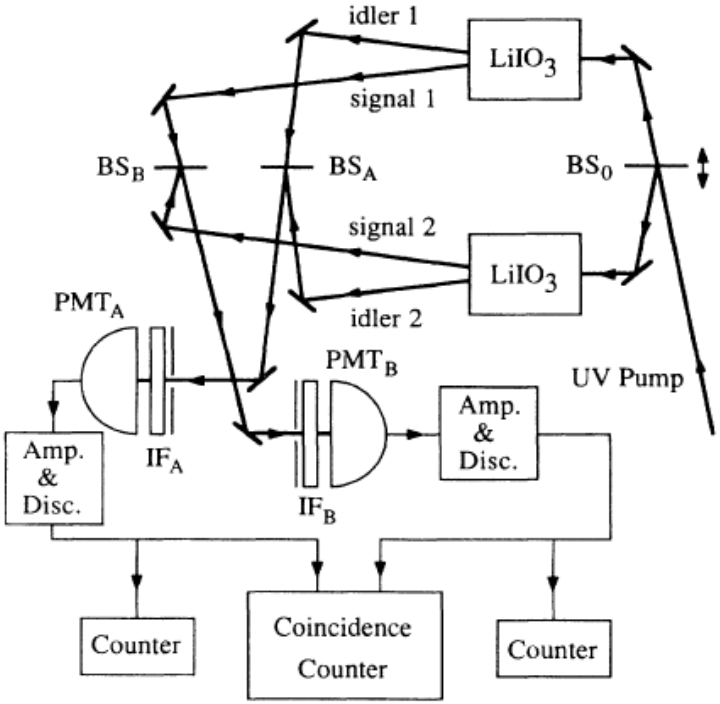

FIG. 2. The setup used in the experiment.

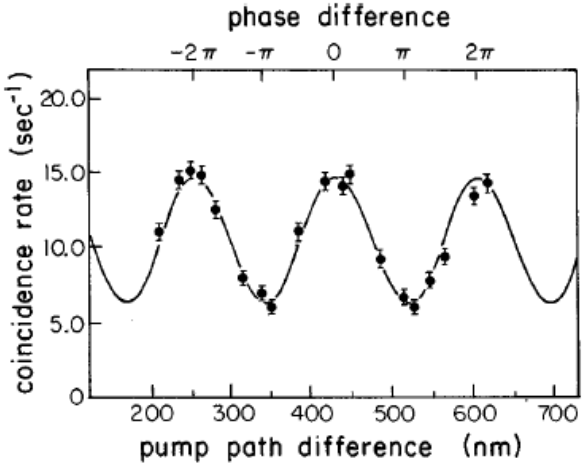

FIG. 5. Results of coincidence measurements by D_A and D_B in Fig. 3 as a function of path difference, showing two-photon interference. The continuous curve is theoretical.

Induced Coherence and Indistinguishability in Optical Interference

X. Y. Zou, L. J. Wang, and L. Mandel

Department of Physics and Astronomy, University of Rochester, Rochester, New York 14627

(Received 18 March 1991)

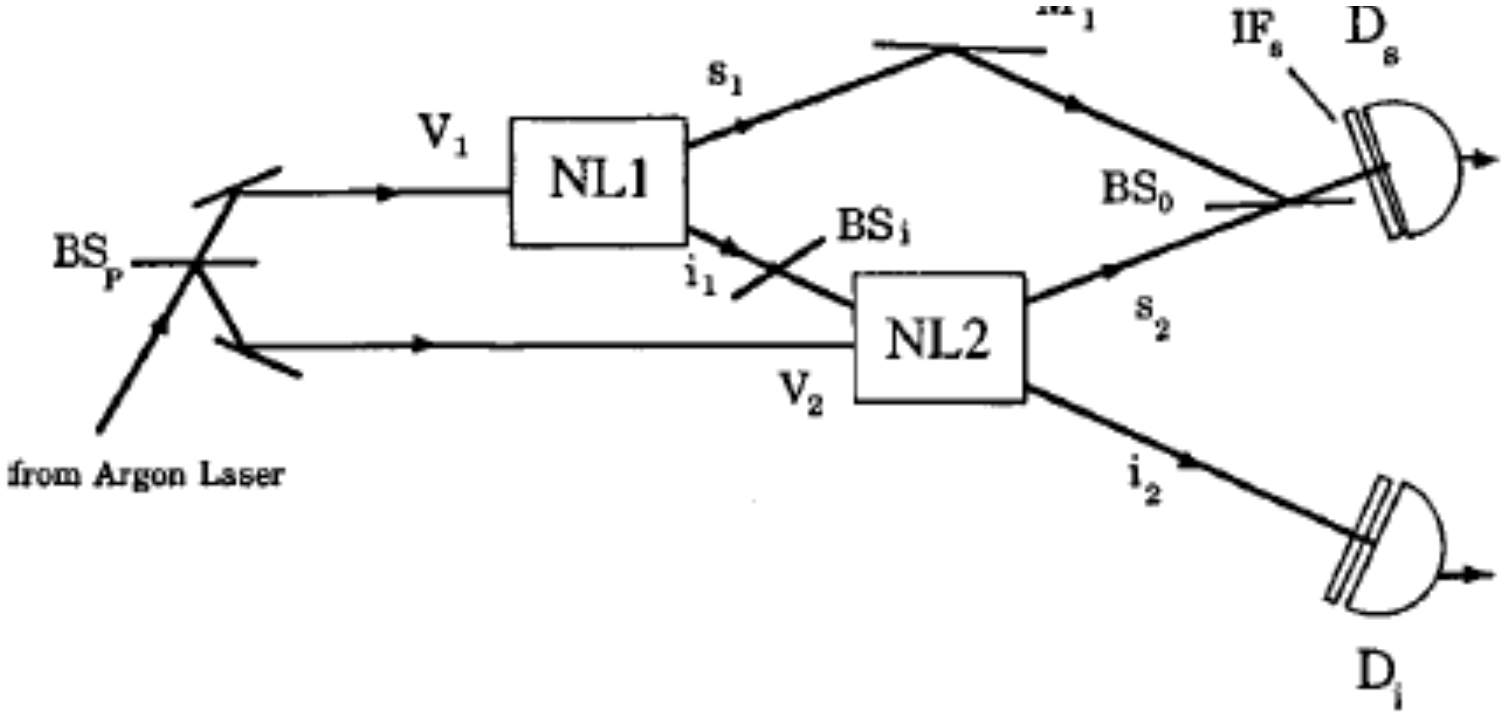

Induced Coherence and Indistinguishability in Optical Interference

X. Y. Zou, L. J. Wang, and L. Mandel

Department of Physics and Astronomy, University of Rochester, Rochester, New York 14627

(Received 18 March 1991)

Second-order interference is observed in the superposition of signal photons from two coherently pumped parametric down-converters, when the paths of the idler photons are aligned. The interference exhibits certain nonclassical features; it disappears when the idlers are misaligned or separated by a beam stop. The interpretation of this effect is discussed in terms of the intrinsic indistinguishability of the photon paths.

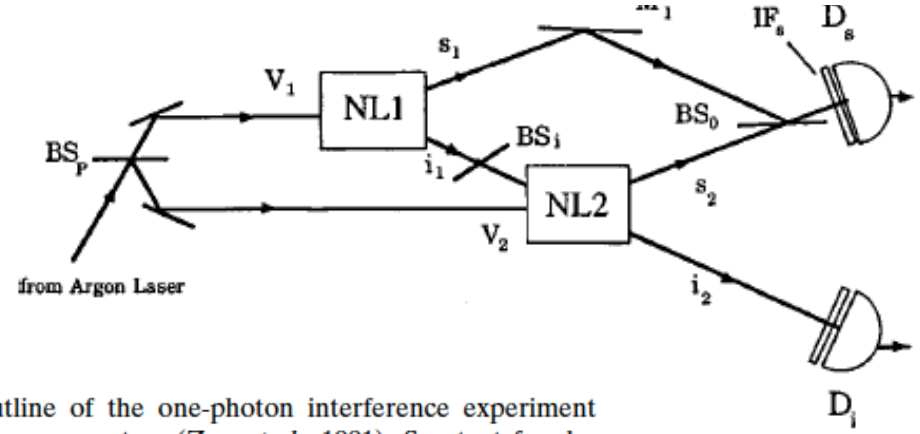

FIG. 6. Outline of the one-photon interference experiment with two downconverters (Zou *et al.*, 1991). See text for description.

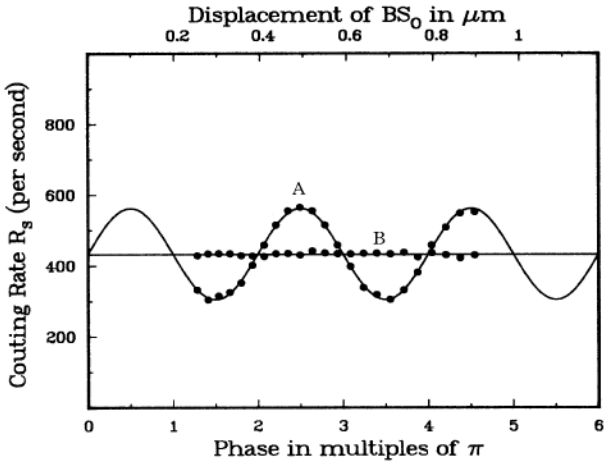

FIG. 2. Measured photon counting rate R_s as a function of beam-splitter BS$_O$ displacement. Curve *A*: neutral-density filter with $|\mathcal{T}|=0.91$ between NL1 and NL2; curve *B*: beam stop with $\mathcal{T}=0$ inserted between NL1 and NL2. 1 standard deviation is smaller than the dot size. The solid curves are the best-fitting sinusoidal functions of period 394 nm.

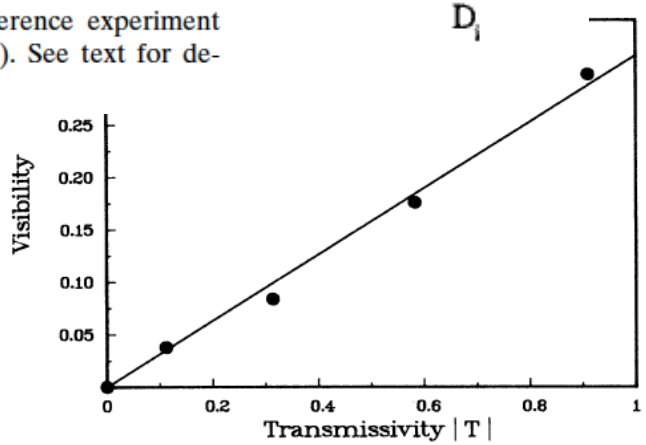

FIG. 3. Measured visibility $\mathcal{V}$ of the second-order interference pattern as a function of amplitude transmissivity $|\mathcal{T}|$ of the filter placed between NL1 and NL2. The uncertainties are comparable with or smaller than the dot size.

Propagation of transient quantum coherence

L. J. Wang and J.-K. Rhee
NEC Research Institute, Inc., 4 Independence Way, Princeton, New Jersey 08540
(Received 23 January 1998; revised manuscript received 18 August 1998)

We perform a time-resolved quantum interference experiment based on the effect of induced coherence without induced emission using two pulsed parametric down-conversion sources. We periodically vary the transmission of the first source's idler beam and measure the time-dependent visibility of fringes in the interference between the two signal beams. The visibility is found to be correlated with the transmissivity with a time delay corresponding to a combined path of the first idler and the second signal beam. The experiment is discussed in the context of the delayed choice experiments. [S1050-2947(99)09402-0]

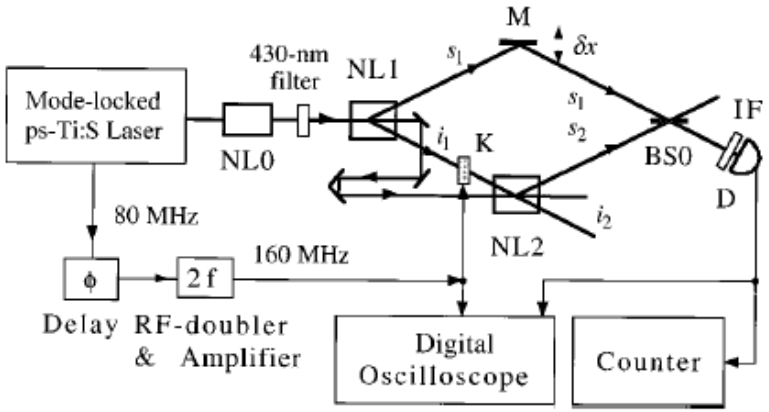

FIG. 1. Schematic setup of the experiment.

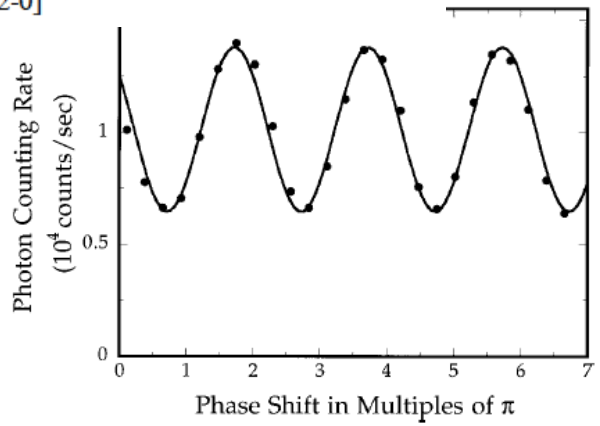

FIG. 2. Typical interference pattern recorded with the avalanche photodiode, *D*. The optical phase shift is introduced by moving the mirror *M*. One standard deviation is smaller than the dot size. The solid curve is the least-squares-fitting sinusoidal of period 860 nm.

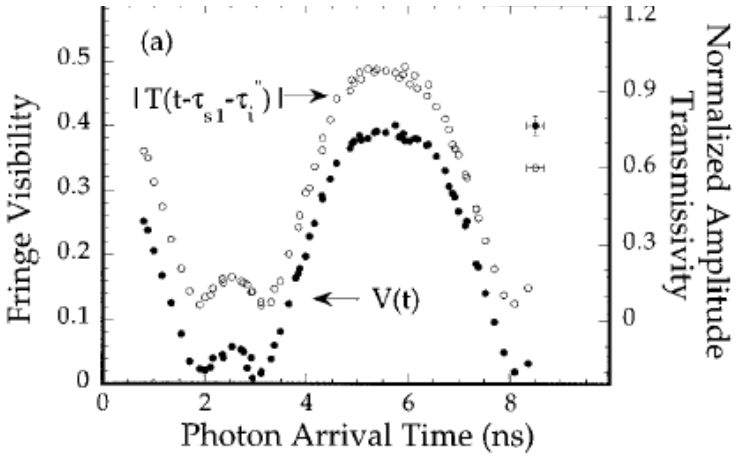

FIG. 3. (a) Time-dependent fringe visibility and the EO modulator's amplitude tramsmissivity. Here the horizontal axis is time relative to the 160 MHz signal that drives the EO modulator. The visibility $V(t)$ (dots) is extracted from the fringes exhibited by photons arriving at the detector at time t. The EO's amplitude transmissivity at an earlier time $(t-\tau_{s2}-\tau_i'')$ is also shown (open circles). Error bars on the right corner represent one standard deviation. (b) Fringe visibility $V(t)$ vs the amplitude transmissivity $|T(t-\tau_{s2}-\tau_i'')|$. The straight line is the least-squares fit.

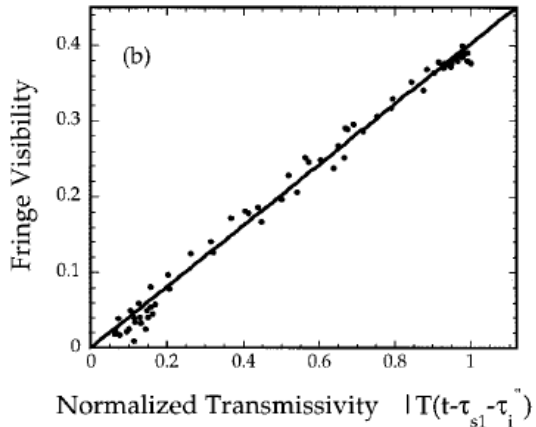

Measurement of the Photonic de Broglie Wavelength of Entangled Photon Pairs Generated by Spontaneous Parametric Down-Conversion

Keiichi Edamatsu, Ryosuke Shimizu, and Tadashi Itoh

Division of Materials Physics, Graduate School of Engineering Science, Osaka University, Toyonaka 560-8531, Japan

(Received 21 February 2002; published 4 November 2002)

Using a basic Mach-Zehnder interferometer, we demonstrate experimentally the measurement of the photonic de Broglie wavelength of entangled photon pairs (biphotons) generated by spontaneous parametric down-conversion. The observed interference manifests the concept of the photonic de Broglie wavelength. We also discuss the phase uncertainty obtained from the experiment.

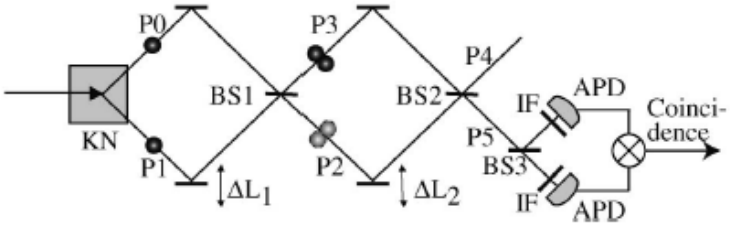

FIG. 1. Schematic experimental setup of the biphoton interference. KN: $KNbO_3$ crystal, BS1 ~ 3: beam splitters, IF: interference filters, APD: avalanche photodiodes.

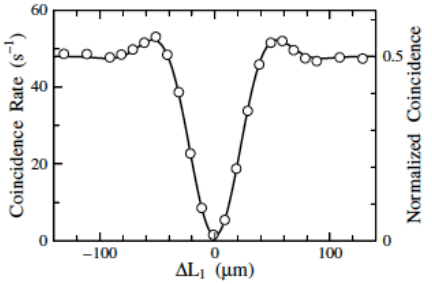

FIG. 2. Coincidence-photon-counting rate detected at the two output ports of BS1 as a function of the optical path-length difference (ΔL_1) between the two paths from KN and BS1 in Fig. 1. Open circles indicate experimental data, and the solid curve is a fitted function that assumes the observed photons have a rectangular spectral shape.

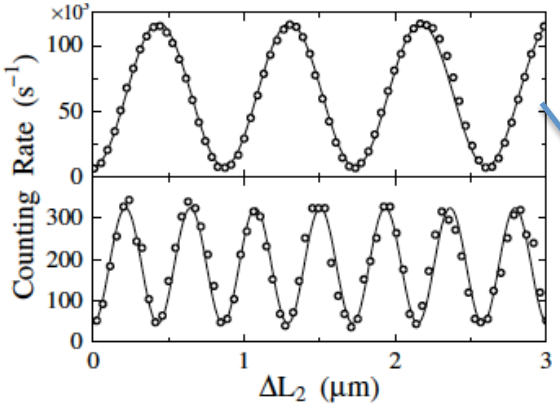

FIG. 3. Interference patterns in the one-photon (upper) and two-photon (lower) counting rates at a path-length difference of around 0 μm.

Block P1 (only 1 photon input)

{No single-photon interference with |1,1> input.}